Potential Energy Surfaces for Chemical Reactions: An Analytical Representation from Coarse Grained Data with an Application to Proton Transfer in Water

Camilla Minichino*,† and Gregory A. Voth*,‡

Department of Chemistry, University of Pennsylvania, Philadelphia, Pennsylvania 19104-6323

Received: December 18, 1996; In Final Form: April 9, 1997[⊗]

In this paper we address the issue of how to represent the potential energy surfaces that arise in chemical reactions from coarse grained electronic structure calculations. Using a reductionistic method based on the reaction surface model, we develop a computational protocol which combines tensor product spline fitting with bivariate interpolation. This approach is particularly useful when one wishes to retain a high degree of accuracy for a few special degrees of freedom. An application of the procedure has been developed for the transfer of a proton between two water molecules. Starting from MP2/6-311G** calculations on $H_5O_2^+$ dimer, we construct the global potential energy surface governing the proton transfer as well as the pattern of charge distributions. In order to study large reactive systems embedded in an external medium, we show how a less demanding procedure can be implemented. It rests on a minimum coupling approach of second-order Taylor expansions of the potential about quasi-stationary points. The resulting potential energy surface is termed a "minimum coupling potential".

1. Introduction

Many aspects of the catalysis and control of chemical reactions are understood on a reasonable qualitative level. But, at the same time, much effort is presently devoted to characterizing and describing the detailed dynamical pathways with the aim of understanding of the overall process in terms of its constituent elementary steps, i.e., of the reaction mechanism. The notion of mechanism is strictly related to the notion of molecular structure in that any reactive process can be represented by nuclear displacements of the molecular system in going from the reactant to the product state. These displacements are described in terms of a suitable set of coordinates, which define a multidimensional nuclear configuration space. At the heart of the description of molecular structure lies a mathematical object: the potential energy surface (PES). It might be considered an oversimplification of reality and an artifact of the Born−Oppenheimer approximation; however, in a conceptual sense, a PES is more than a mathematical object because most chemical phenomena are best understood in terms of it.

From a computational point of view, the nature of a PES can be probed, with increasing accuracy, using *ab initio* quantum chemical calculations. But those calculations yield coarse grained information: one only knows the values assumed by the potential energy at many nuclear configurations. The need for developing analytical representations of the PES that are determined from electronic structure calculations arises because they are sufficiently time consuming that the explicit computation of energies and energy gradients at every point needed in a dynamics study is rarely feasible. In addition, the knowledge of the functional form of the PES provides building blocks which enable to construct—by a blending procedure—the PES for more complex systems or systems embedded in a medium.

A full PES can be obtained by either fitting an assumed global functional form to the data or by interpolating in some manner between the known data points (see, e.g., refs 1−5). Several methods have been developed to treat accurately small polyatomic systems; however, their *brute force* extension to large molecules is in practice not feasible. The only solution is to take recourse to a basic concept of scientific methods: reductionism (see, e.g., ref 6). In this vein the strategy to adopt is (1) restriction to the PES governing a particular process and (2) limitation to that part of the nuclear configuration space which is energetically relevant, i.e., the reaction path and its immediate environment.

The general reaction path concept (ref 7 and references therein), together with some specific definition of it in terms of the natural collision coordinate[8] and the intrinsic reaction coordinate[9] and with the reaction path Hamiltonian approach of Miller et al.,[10] provides an invaluable reference framework in the theoretical description of several processes. However the study of some reactions, e.g., proton transfers, requires a revision and extension of the reaction path model. Such kinds of processes can be seen as the polyatomic version of the simplest model of a chemical reaction, a collinear atom−diatom system, e.g., $X + HY \rightarrow XH + Y$, where X and Y are heavy atoms. The difficulty in describing this "heavy + light-heavy" mass combination by a single, even global, coordinate like the intrinsic reaction coordinate is well known. And it is furthermore known that the tunneling dynamics does not follow the path corresponding to the reaction coordinate but rather "cuts the corner", the linear path being the extreme version of this.

Another problem arises if one aims to use a "gas phase" PES obtained by a reaction path approach as a core potential of the overall PES for a proton transfer process in a generic external medium. The medium, even if not actively participating in the reaction, alters the reaction path. Also, a PES built in terms of the gas phase reaction path may not be intrinsically suitable to correctly describe such modulation effects due to the medium. The above drawbacks could be avoided by adopting a more flexible approach: the reaction surface model. However, its practical use has been limited by two factors: high computational cost in obtaining the *ab initio* data and difficulty in expressing them in an appropriate and general functional form. In this work we present a strategy to overcome the latter problem and to minimize the first.

† Permanent address: Dipartimento di Chimica, Università della Basilicata, via N. Sauro 85, I-85100 Potenza, Italy. E-mail: minichino@unibas.it.

‡ Present address: Department of Chemistry, University of Utah, Salt Lake City, UT 84112. E-mail: voth@chemistry.chem.utah.edu.

⊗ Abstract published in *Advance ACS Abstracts,* May 15, 1997.

S1089-5647(97)00036-9 CCC: $14.00 © 1997 American Chemical Society

Our approach uses Taylor expansions about topologically relevant points of the nuclear configurations space. Therefore, it can be framed in the methodologies for global PESs (see, e.g., refs 11−15) which aim to exploit the present status of the art of electronic structure calculations: the easiness in obtaining pointwise information not only for the PES value but also for its shape.

The present paper is organized as follows: in section 2 we revise the reaction surface model, whereas in section 3 we present two approaches for its application to complex systems. In the first one the parameters entering in the reaction surface model are obtained by means of tensor product spline fitting and bivariate interpolation. In the second one we suggest to adopt the minimum coupling (MC) method, i.e., a method originally proposed for building a PES by using Taylor expansions limited to minima and saddle points,[11] for an approximate evaluation of the coefficients obtained in the first approach through bivariate interpolation. As an application, in section 4 we construct the PES for the proton transfer between hydronium and water, adopting two limiting models based on local Taylor expansions: namely, the original MC method and the spline fitting plus bivariate interpolation approach to the reaction surface PES. Conclusions are then given in section 5.

2. General Model: Adiabatic Reaction Surface

First, some remarks are in order regarding the notation used. Bold characters are used to indicate arrays, superscripts enclosed in parentheses specify the order of the derivative of a function with respect to the variables on which it depends, and the "t" superscript means the transpose of an array.

Let us consider an M-body (nonlinear) system and a vector $\mathbf{q}$ whose $N = 3M - 6$ $\{q_1, ..., q_N\}$ components are the generalized internal coordinates which uniquely describe each nuclear arrangement. These coordinates can be partitioned in two subsets composed of two *acting* ($\mathbf{r}$) and $N - 2$ *spectator* ($\mathbf{u}$) coordinates, respectively. The choice of the $\mathbf{r}$ elements is crucial in that they must describe the essential characteristics of the large amplitude (reactive) motion which brings the system from the reactant to the product state. They are therefore not specific to the system but to the reaction channel under analysis. In particular, for proton transfer processes, the elements of $\mathbf{r}$ can be considered to be the donor/acceptor distance and a coordinate describing the location of the transferring proton. In contrast, any set of spectator $\mathbf{u}$ coordinates complementing $\mathbf{r}$ to $\mathbf{q}$ is assumed to be more or less adequate: they only act as an intracomplex "bath" which influences the exchange of energy among the active coordinates. Such transfers can be more effective if the bath adiabatically follows the reactive event, i.e., if the $\mathbf{u}$ coordinates depend parametrically on $\mathbf{r}$, where the physical nature of their interconnection must still be specified.

With the above considerations in mind, a reaction can be described in terms of the motion on the large amplitude surface—which is a function of the active coordinates and of the quasi-equilibrium values $\bar{\mathbf{u}}$ assumed by the bath coordinates when they adiabatically follow the large amplitude motions—and the deviations away from it. Therefore, following Carrington and Miller,[16] the overall potential energy surface can be approximated by expanding the $\mathbf{u}$ dependence to the second order in $\bar{\mathbf{u}}$

$$V(\mathbf{q}) \approx V(\mathbf{r},\mathbf{u}) = \bar{V}(\mathbf{r}) + [\mathbf{u} - \bar{\mathbf{u}}(\mathbf{r})]^t \cdot \mathbf{V}_{\mathbf{u}}^{(1)}(\mathbf{r}) + {}^1/_2[\mathbf{u} - \bar{\mathbf{u}}(\mathbf{r})]^t \cdot \mathbf{V}_{\mathbf{uu}}^{(2)}(\mathbf{r}) \cdot [\mathbf{u} - \bar{\mathbf{u}}(\mathbf{r})] \quad (2.1)$$

where

$$\bar{V}(\mathbf{r}) = V[\mathbf{r},\bar{\mathbf{u}}(\mathbf{r})] \quad (2.2)$$

also contains the self-interaction of the $\mathbf{u}$ coordinates. The function $\bar{V}(\mathbf{r})$ is the surface where most of the reactive event takes place, whereas

$$\mathbf{V}_{\mathbf{u}}^{(1)}(\mathbf{r}) = \left(\frac{\partial V(\mathbf{r},\mathbf{u})}{\partial \mathbf{u}}\right)_{\mathbf{u}=\bar{\mathbf{u}}(\mathbf{r})} \quad (2.3)$$

and

$$\mathbf{V}_{\mathbf{uu}}^{(2)}(\mathbf{r}) = \left(\frac{\partial^2 V(\mathbf{r},\mathbf{u})}{\partial \mathbf{u}\, \partial \mathbf{u}}\right)_{\mathbf{u}=\bar{\mathbf{u}}(\mathbf{r})} \quad (2.4)$$

are the first and second derivatives of the energy with respect to the bath coordinates evaluated at $\bar{\mathbf{u}}$.

In any kind of dynamical study the low-energy part of the PES which contains reactant and product configurations is certainly explored, and the reduced surface $\bar{V}$ must belong to this region. In order to locate it, one can take recourse to some variational criterium: i.e., it may be the gradient extremal surface[17−19] or a minimum energy surface. In this last case $\bar{V}$ is defined by minimizing the potential energy of the system with fixed values of $\mathbf{r}$. This leads to the vanishing of the linear term in $[\mathbf{u} - \bar{\mathbf{u}}(\mathbf{r})]$ and the equation

$$\partial V(\mathbf{r},\mathbf{u})/\partial \mathbf{u} = 0 \quad (2.5)$$

determines $\bar{\mathbf{u}}(\mathbf{r})$. It should be noted that the above equation is less restrictive than the condition $\partial V/\partial \mathbf{q}$ which defines the stationary points. Hence all stationary points from reagents to products (saddle point for transition states and potential minima for equilibrium configurations) belong to $\bar{V}$.

If the parameters entering into eq 2.1 are fitted to a functional form, one has a global PES which can be used in dynamical studies. Also the computation of forces (i.e., the negative of the energy gradient) is a simple task: the Cartesian first derivatives of the PES ($\mathbf{G}$) can be computed numerically by finite differences of the energy or obtained in terms of its curvilinear counterpart $\mathbf{g}$ (which is in turn easily determined by taking the first derivative of the reaction surface function) by using the equation

$$\mathbf{G} = \mathbf{B}^t \cdot \mathbf{g} \quad (2.6)$$

where the elements of the so-called $\mathbf{B}$ matrix express the variation of the internal coordinates with infinitesimal Cartesian displacements.[20,21] Implicit in the above equation is the fact that the surface $\bar{V}(\mathbf{r})$ will usually need to be expressed in terms of some curvilinear internal coordinates for an accurate global representation.

According to the present model, the first step in obtaining a global PES is the selection of the two sets of coordinates. The variational criterium to follow for individuating $\bar{V}$ may be dictated by practical convenience. In fact, due to the effectiveness of gradient optimization algorithms which are implemented in current electronic structure packages, the minimum energy surface choice is the most easy to pursue. This choice uniquely characterizes the adiabatic bidimensional surface. The next step is to carry out constrained geometry optimizations over a two dimensional grid of $n = n_{r_1} n_{r_2}$ pairs of values for the reaction surface variables r_1 and r_2. Successively, the Hessian matrices at such points must be computed. A set of values for $\bar{V}$, quasi-equilibrium (minimized) bath coordinates $\bar{\mathbf{u}}$, and reduced Hessian $\mathbf{V}_{\mathbf{uu}}^{(2)}$ is obtained. Finally, the data must be fitted to a functional form.

In addition to the heavy computational cost of electronic structure calculations, the determination of the parameters entering into eq 2.1 also implies that a very large number of fittings must be performed. Particularly troublesome is to set the $(N-2)[(N-1)/2]$ elements which uniquely determine the reduced Hessian. An alternative can be the reduction of the N-dimensional system to an effective bidimensional one, and this has been accomplished[16,22] by making proper approximations also on the kinetic energy terms of the system. If such approximations are not made, one has to deal with a large number of data fittings; hence a reliable and effective computational protocol must be developed.

3. Computational Methods

A. Spline Fitting and Bivariate Interpolation. The first problem to address is the choice of the analytical expression for the interpolating functions. Several classes of functions can be used, e.g., polynomial, Morse, Padé approximants, or *ad hoc* functions may be suggested by the trend of the data. However, the effort required in obtaining a given accuracy of fit can strongly depend on the functional form chosen, and as a consequence, and if a more general PES is to be built, each variable to be fitted may require a particular treatment. In order to deal with this problem, one can use spline functions (i.e., piecewise polynomials) whose effectiveness in data interpolation is well known.[23,24] Compared with ordinary polynomials, spline functions are far more flexible; they are able to deal with local behavior. Additional boundary constraints which can often significantly improve the quality of the fit are easily implemented. In particular, we have used here tensor product B-splines as approximating functions. Such an approach to multivariate interpolation is efficient only when the data values are specified at nodes of a rectangular mesh, i.e., if one has data values $F(i,j)$ corresponding to data points $\{r_1(i), r_2(j); i = 1, ..., n_1; j = 1, ..., n_2\}$. However this is not a limitation in our case: *ab initio* data can always be generated (or recast) in such form. For each function to fit, the parameters to be determined are the degree of the splines, the number and the position of the knots, and the coefficients of the interpolant. Bicubic splines give a good compromise between efficiency and quality of the fit.[23] The position and number of knots are set in an adaptive way:[24] more knots are located in those regions where the function underlying the data is difficult to approximate than where it has a smooth behavior.

By using bicubic spline fitting one can then get a functional form for the adiabatic reaction surface and for the quasi-equilibrium bath coordinates. For the elements of the reduced Hessian, we instead use an alternative approach: a bivariate interpolation over a sparse grid. In practice, if one knows the value of $\mathbf{V}_{\mathbf{uu}}^{(2)}$ over a set $\{r_1(i), r_2(j); i = 1, ..., \nu_1; j = 1, ..., \nu_2\}$ of $\nu_1 \ll n_1$ and $\nu_2 \ll n_2$ points for the $\mathbf{r}$ variables, its value for a nuclear configuration in the range $[r_1(i), r_1(i+1)] \times [r_2(j), r_2(j+1)]$ can be determined by a four point formula[25]

$$\begin{aligned}\mathbf{V}_{\mathbf{uu}}^{(2)}[r_1(i)+ph, r_2(j)+qk] = (1-p)\times \\ (1-q)\mathbf{V}_{\mathbf{uu}}^{(2)}[r_1(i), r_2(j)] + p(1-q)\mathbf{V}_{\mathbf{uu}}^{(2)}[r_1(i+1), r_2(j)] + \\ q(1-p)\mathbf{V}_{\mathbf{uu}}^{(2)}[r_1(i), r_2(j+1)] + pq\mathbf{V}_{\mathbf{uu}}^{(2)}[r_1(i+1), r_2(j+1)]\end{aligned} \tag{3.1}$$

where h and k are the spacing between consecutive points of the mesh along the r_1 and r_2 axes, respectively.

Although the reduced Hessian is not treated as accurately as the other parameters entering in eq 2.1, one should note that the effect of the spectator modes on the PES also depends on the quasi-equilibrium bath coordinates. If one analyzes the constraint equation which determines these last quantities, it is evident that they contain information on the "true" reduced Hessian around $\mathbf{r}$. Let us consider, for example, the case in which the bidimensional surface is defined by a minimum energy criterium and therefore the variation of the $\bar{\mathbf{u}}$ with $\mathbf{r}$ is defined by eq 2.5. By differentiating this equation with respect to $\mathbf{r}$, one obtains

$$\frac{\partial \bar{\mathbf{u}}}{\partial \mathbf{r}} = -\frac{1}{\mathbf{V}_{\mathbf{uu}}^{(2)}} \cdot \mathbf{V}_{\mathbf{ru}}^{(2)} \tag{3.2}$$

Thus $\bar{\mathbf{u}}$ at $\mathbf{r}$ is related to $\bar{\mathbf{u}}$ at $\mathbf{r} - \Delta\mathbf{r}$ by the following equation

$$\bar{\mathbf{u}}(\mathbf{r}) \approx \bar{\mathbf{u}}(\mathbf{r}-\Delta\mathbf{r}) - \frac{1}{\mathbf{V}_{\mathbf{uu}}^{(2)}(\mathbf{r}-\Delta\mathbf{r})} \cdot \mathbf{V}_{\mathbf{ru}}^{(2)}(\mathbf{r}-\Delta\mathbf{r}) \cdot \Delta\mathbf{r} \tag{3.3}$$

where

$$\mathbf{V}_{\mathbf{ru}}^{(2)}(\mathbf{r}) = \left(\frac{\partial^2 V(\mathbf{r},\mathbf{u})}{\partial \mathbf{r}\, \partial \mathbf{u}}\right)_{\mathbf{u}=\bar{\mathbf{u}}(\mathbf{r})} \tag{3.4}$$

Because of this, the parametrized values of $\bar{\mathbf{u}}$ over the range of $\mathbf{r}$ carry information on the exact Hessian matrix.

The computational protocol sketched above has been applied in computing the PES for the proton transfer reaction in the $H_5O_2^+$ dimer (see section 4).

B. Minimum Coupling Approximation. The extension of the above method to very large systems becomes problematic considering the high computational cost implicit in the evaluation of several Hessian matrices. In order to overcome this problem, one can take recourse to a method generally known as the empirical valence bond method which was originally developed by Warshel[26] to obtain a reasonable estimate of the PES for very large (condensed phase or biomolecular) systems. Subsequently, Chang and Miller[11] reformulated and recast it in order to fully exploit the present state of the art for electronic structure calculations. Such an approach, when further generalized, can provide nonlocal information by applying a minimum coupling principle to properly selected local information; we thus prefer to refer to it as a minimum coupling method. Below such a method is cast in a broad perspective and shown how it can be used for our present goal: an economical, albeit reliable, approximation of the restricted Hessian entering into eq 2.1 in order to treat very large systems.

Following the view of Fukui,[27,28] one can envisage the configuration space corresponding to a molecular system as a series of cells. Each cell contains a minimum energy configuration, and saddle points are located at the intercell boundaries. To each cell one can associate a local, or diabatic, potential which may be approximated by the Taylor expansion $T_k(\mathbf{q})$ about the minimum-like configuration $\mathbf{q}_k$ contained in it

$$T_k(\mathbf{q}) = V(\mathbf{q}_k) + \delta\mathbf{q}_k^t \cdot \mathbf{V}^{(1)}(\mathbf{q}_k) + {}^1/_2 \delta\mathbf{q}_k^t \cdot \mathbf{V}^{(2)}(\mathbf{q}_k) \cdot \delta\mathbf{q}_k + ... \tag{3.5}$$

where $\delta\mathbf{q}_k$ is the difference between $\mathbf{q}$ and $\mathbf{q}_k$. The zeroth-order coefficient defines the center of the cell, and the higher ones characterize its shape. The overlap of a cell to its neighbors depends on the mutual couplings. The adiabatic potential is that surface that smoothly joints one cell to another, i.e., the one for which the couplings are zero and keeps the lowest, V_{MC}, of its possible values. Such a conceptual scenario however, must be translated into mathematical terms, and this is now done.

Let us first introduce a generic potential energy operator $\hat{v}(\mathbf{q})$ and a set of states for each minimum-like nuclear configuration assumed by the system in going from a given initial state to the final one. This operator can be defined in a discrete way by its matrix representation ($\mathbf{v}$) on a finite basis set of states. Each diagonal element represents the cell potential for the $|k\rangle$ state

$$v_{kk}(\mathbf{q}) = \langle k|\hat{v}(\mathbf{q})|k\rangle \equiv T_k(\mathbf{q}) \tag{3.6}$$

whereas each kl-th off-diagonal element (i.e., the coupling between cells) is expressed as a function, for the moment unknown, of the diabatic potentials relative to the k, l-th pair

$$v_{kl}(\mathbf{q}) \equiv v_{lk}(\mathbf{q}) = \langle k|\hat{v}(\mathbf{q})|l\rangle = C\,(v_{kk}(\mathbf{q}), v_{ll}(\mathbf{q})) = C(\mathbf{q})_{kl} \tag{3.7}$$

In the following, we omit the explicit dependence on $\mathbf{q}$, unless necessary to avoid confusion.

The coupling functional must be modeled to describe atomic rearrangements that lead the system from the configuration $\mathbf{q}_k$ to $\mathbf{q}_l$, and can be defined by the following condition

$$C_{kl}^2 \equiv B_{kl} = (v_{kk} - V)(v_{ll} - V) \tag{3.8}$$

where $V \equiv V(\mathbf{q})$ is the exact potential; therefore it vanishes when one or both cell potentials coincide with the full potential, namely in the area of the minima. However, one has to impose a correct asymptotic behavior so that the coupling is effective only for $\mathbf{q}$ belonging to the closed range $[\mathbf{q}_k,\mathbf{q}_l]$ (see Appendix A). Now the functional relation in eq 3.8 must be transformed into an explicit function of $\mathbf{q}$. To do so, one substitutes for the diabatic potentials their approximate forms: the known Taylor expansions with coefficients derived by electronic structure calculations which may be also corrected to reproduce some experimental data. The exact potential $V(\mathbf{q})$ is an unknown quantity. However, by taking an additional point $\mathbf{q}_{kl}$ belonging to the same closed range points, we can approximate it by the Taylor expansion about $\mathbf{q}_{kl}$

$$V(\mathbf{q}) \approx V(\mathbf{q}_{kl}) + \delta\mathbf{q}_{kl}^t\cdot\mathbf{V}^{(1)}(\mathbf{q}_{kl}) + {}^1/_2\delta\mathbf{q}_{kl}^t\cdot\mathbf{V}^{(2)}(\mathbf{q}_{kl})\cdot\delta\mathbf{q}_{kl} + ... \tag{3.9}$$

whose parameters can be obtained by *ab initio* calculations. This approximation together with the form chosen for the diabatic potentials, yields an approximation to the function $B_{kl}(\mathbf{q})$ in eq 3.8 (see Appendix A). The location of $\mathbf{q}_{kl}$ establishes the junction between the two cells and can be chosen to be at the saddle point or roughly halfway between them. In view of the availability of first and second derivatives of the energy in electronic structure packages, for practical applications Taylor series truncated to second order are chosen. In Appendix A we report more details about the coupling function.

The minimum coupling potential (MCP) can be identified as the lowest eigenvalue, V_{MC}, of the matrix representation of $\hat{v}$. Hence, once the elements of $\mathbf{v}$ are known, a symbolic diagonalization is the last step to obtain the analytical expression of V_{MC}. Since a reaction involving a single bistable system leads to a 2 by 2 $\mathbf{v}$ matrix, such a diagonalization is a simple task (see Appendix B).

A more accurate MCP would entail the evaluation of high-order terms of the Taylor expansions on which it depends, e.g., at least for the hydrogen bond coordinate in a proton transfer complex. However, this is not enough if one would like to use the gas phase MCP to set the potential of, e.g., an intermolecular hydrogen bond dimer in a polar environment. The interactions between dimer and medium lead to a perceptable variation of the donor/acceptor distance in the dimer. Therefore Taylor expansions about the equilibrium points of the gas phase system are not suited in describing the local environment of the equilibrium points of the solvated dimer. On the basis of such considerations, an alternative can be found in treating the hydrogen bond and donor/acceptor coordinates of the dimer so to use the minimum coupling method based on second-order Taylor expansions only to evaluate the corrective effect of the remaining degrees of freedom. Such a separation between sets of coordinates is the idea at the heart of the approach described in the previous section. Therefore, coming back to eq 2.1, we rewrite it as

$$V(\mathbf{q}) \approx V\,(\mathbf{r},\mathbf{u}) = \bar{V}(\mathbf{r}) + [\mathbf{u} - \bar{\mathbf{u}}(\mathbf{r})]^t\cdot\mathbf{V}_{\mathbf{u}}^{(1)}(\mathbf{r}) + {}^1/_2[\mathbf{u} - \bar{\mathbf{u}}(\mathbf{r})]^t\cdot\mathbf{V}'^{(2)}_{\mathbf{uu}}(\mathbf{r})\cdot[\mathbf{u} - \bar{\mathbf{u}}(\mathbf{r})] \tag{3.10}$$

where $\mathbf{V}'^{(2)}_{\mathbf{uu}}(\bar{\mathbf{u}}_k)$ is the *minimum coupling approximation* to the reduced Hessian in eq 2.1.

In order to determine $\mathbf{V}'^{(2)}_{\mathbf{uu}}(\bar{\mathbf{u}}_k)$, one has to first select the $\mathbf{q}_k$ and $\mathbf{q}_l$ points for the cell potentials. A common feature of the PES in hydrogen-bonded systems is the presence of two merging valleys whose depth increases with the distance between the acceptor and donor entities. In order to define the two local potentials, one can expand about points chosen in the following way: the positions on the minima which correspond to the donor/acceptor distance, which is in the middle of the relevant range, would be used as the center points of the diabatic potentials. A point $\mathbf{q}_{kl}$ on the ridge between them can be used to define the coupling potential. Once the location of the σ-th (with $\sigma = k, l, kl$) points is fixed, the diabatic potentials and coupling function can be set through *ab initio* data. This in turn yields the MC approximation of the potential (see Appendix B, eq B2). Next, by virtue of eq B5, the analytical expression of the MC Hessian is obtained. Finally, discarding the rows and columns corresponding to the active modes $\mathbf{r}$, one gets $\mathbf{V}'^{(2)}_{\mathbf{uu}}$.

4. Applications

We now show two examples of how local Taylor expansions about a certain set of points can be combined to obtain a global PES. In the first subsection we use a minimal number of Taylor expansions, namely those about the stationary points involved in the reaction channel under analysis. They are then combined, according to eq B2, to give the global PES. In the second subsection, instead, we use an extended set of Taylor expansions about nuclear configurations which are topologically relevant. They in fact lie on the bidimensional minimum energy surface where most of reactive process is thought to take place. Then, by means of bidimensional spline fittings and bivariate interpolation, one obtains an analytical representation for the PES of eq 2.1.

All the electronic structure calculations for determining the Taylor expansion coefficients were performed by using the Gaussian 94 package.[29]

A. Test of the MC Method for Proton Transfer. Although a MCP has been successfully used in a classical trajectory study of the reaction $H_2CO \rightarrow H_2 + CO$,[12] it is of interest to test its reliability in describing proton transfer processes. We have chosen $H_5O_2^+$ (cf. Figure 1) and malonaldehyde as benchmarks because they are different in the type (intermolecular vs intramolecular) and strength (strong vs medium) of the hydrogen bond. At the level of theory used (HF/6-31G**) the barrier minimum−saddle point is 0.15 kcal/mol for $H_5O_2^+$ dimer and 10.25 kcal/mol for malonaldehyde. The terms entering into the

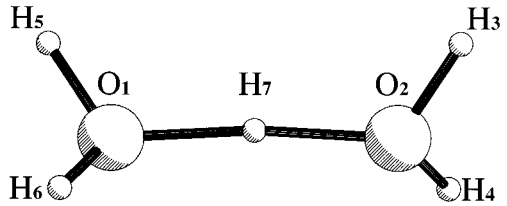

Figure 1. Atom labeling for the $H_5O_2^+$ complex. The geometrical configuration shown corresponds to the MP2/6-311G** minimum.

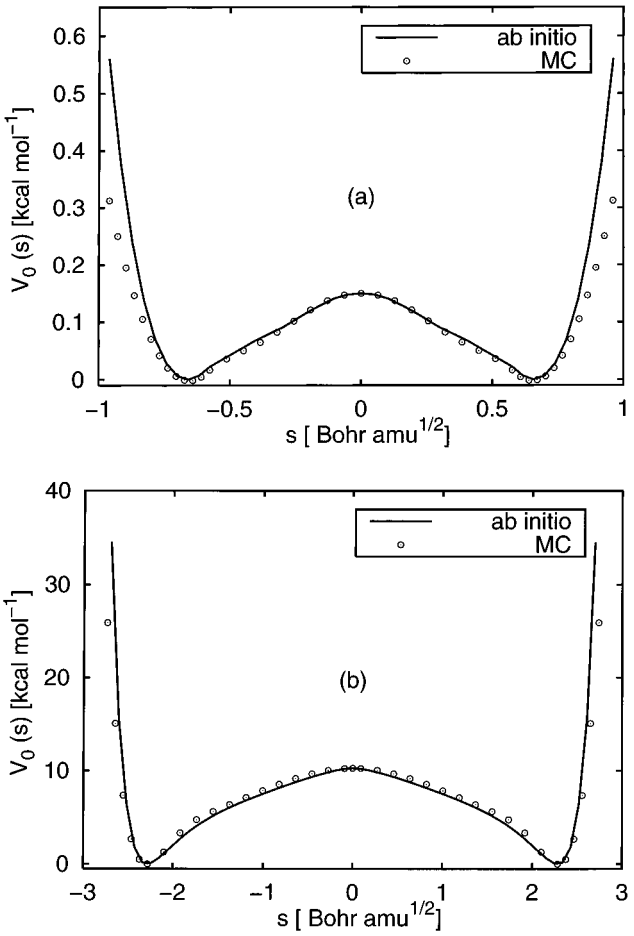

Figure 2. Comparison between minimum coupling (MC) and *ab initio* (HF/6-31G**) minimum potential energy profiles (V_0) for the proton transfer in the (a) $H_5O_2^+$ dimer and (b) malonaldehyde. The path is parametrized in terms of a reaction coordinate *s* which has been chosen to be the signed distance, in mass-weighted Cartesian coordinates, of a point along the path from the saddle point configuration.

expression of the diabatic (eq A1) and coupling potentials (eq A2) were obtained using the *ab initio* data (energy, coordinates, and Hessian) for the minima and saddle points. Then, using eqs B2, B4, and B5, an analytical expression for the MC energy, gradient, and Hessian was obtained. The resulting PES correctly reproduces the location and force field of the stationary points. To probe it on a wider and more significant range we also computed a minimum energy path by fixing the distance of the transferring proton from the donor site and optimizing the remaining degrees of freedom. The path, which passes through the saddle point, has been parametrized in terms of a reaction coordinate (*s*) which has been chosen to be the signed distance, in mass-weighted Cartesian coordinates, of a point along the path from the saddle point configuration. In Figure 2 we compare the *ab initio* and MC potential energy profiles $V_0(s)$ for the two hydrogen bond systems. These curves match in the area minimum−saddle point−minimum, whereas the agreement over the regions beyond the minima is less satisfactory. In the latter zones the coupling term is no longer effective. Thus, the potential corresponds to that of the diabatic cells, which were chosen to be harmonic. Therefore, in order to improve the PES, one should use higher order terms in the Taylor expansions about stationary points or, alternatively, a larger set of second-order Taylor expansions. This latter approach is followed in next application.

B. Fit of the Accurate $H_5O_2^+$ PES. The proton transfer between water and hydronium ion has received considerable attention due to the role such a dimer plays[30] in understanding proton mobility in water. If the gas phase complex is thought of as a solute,[31] the total potential for $H_5O_2^+$ complex in solution can be modeled as a sum of a complex (V_C), a solvent−complex (V_{SC}), and solvent (V_{SS}) potentials, i.e.,

$$V = V_C + V_{CS} + V_{SS} \tag{4.1}$$

In this section we address the issue of analytically representing the complex potential and the parameters necessary to formulate the complex−solvent potential.

Although numerous studies have been devoted to the $H_5O_2^+$ dimer, no global potential—one derived from *ab initio* data—is yet available, at least to our knowledge. Hartree−Fock calculations using small basis sets[32,33] predict a single-well PES, while larger basis sets and polarization functions result in a double-well PES. The addition of correlation up to coupled cluster including single, double, and perturbatively connected triple excitation (CCSD(T))[34] calculations have resulted in general agreement on the symmetric nature of the ground state for the $H_5O_2^+$ system in the gas phase.[35] In view of the extension of the present methodology to larger clusters of hydrated hydronium ions, a balance was sought between the quality and the feasibility of calculations. It has been shown[36] that advanced electron correlation methods lead to results in close agreement with second-order perturbative treatment (MP2). On the basis of such considerations we performed MP2 calculations using the 6-311G** basis set,[37] i.e., a standard valence triple-zeta basis set augmented with a single set of polarization functions. This basis set is flexible enough to give the interaction energy for the $H_5O_2^+$ system in good accordance with larger basis sets.[38] In particular, only five uncontracted d functions are used for polarization functions on oxygen atoms because the use of the full set of six functions introduces an additional s function which to some extent duplicates the properties of part of the sp basis. Furthermore, the correlation energy was limited to the valence atomic orbitals. This choice was made since the 6-311G** basis set was developed by optimizing exponents and coefficients at the MP2 frozen core level and was intended to be used with this approximation.

The minimum energy surface criterium was employed to construct the reaction surface. Constrained geometry optimizations were carried out for 84 different points, where each point corresponds to a specific value of the O_1O_2 and HO_1 distances. (See Figure 1 for atom numbering.) In particular, after selecting the $n_{O_1O_2} = 7$ value of the interoxygen distance ranging from 2.3 to 2.8 Å, the optimized geometrical configurations for the proton halfway between the heavy atoms were determined. Then, for each $n_{O_1O_2}$ value of O_1O_2 and for a decreasing set of H_7O_1 distances, we performed the optimization of the geometry for the off-surface degrees of freedom. The definitions of such geometrical parameters are given in Table 1. We then expressed the data to be fitted as function of the asymmetric stretch, $H_7O_1-H_7O_2(r_1)$, of the transferring proton and of the O_1O_2 (r_2) distance. The use of a symmetry-adapted coordinate for the excess proton is particularly convenient if we want to keep the number of parameters (knots and spline coefficients) entering

TABLE 1: MP2/6-311G Geometrical Parameters for the Minimum Configuration of the $H_5O_2^+$ and $[H_5O_2^+]4H_2O$ Complexes**[a]**

	$H_5O_2^+$	$[H_5O_2^+]4H_2O$
	Bond Lengths (Å)	
O_1O_2*	2.3782	2.3777
H_7O_1*	1.1907	1.1892
H_3O_2	0.9665	0.9839
H_4O_2	0.9661	0.9838
H_5O_1	0.9665	0.9839
H_6O_1	0.9661	0.9838
	Bond Angles (deg)	
$H_3O_2O_1$	122.269	116.100
$H_4O_2H_3$	108.898	108.406
$H_5O_1O_2$	122.269	116.100
$H_6O_1O_5$	108.898	108.406
$H_7O_1O_5$	119.435	114.649
	Dihedral Angles (deg)	
$H_4O_2H_3O_1$	139.300	129.516
$H_6O_1H_5O_2$	139.300	129.516
$H_5O_1O_2H_3$	36.329	18.374
$H_7O_1H_5H_6$	−138.234	−129.258

[a] We only report the parameters of the solvated dimer corresponding to those of the gas phase dimer. The coordinates marked by an asterisk are those used to set the active variables **r**, the remaining ones are the bath coordinates.

in the bivariate fitting low. In general, if the function to be approximated has a difficult feature, a peak say, running along a line parallel to the r_1 axis, then, by proper refinement of the mesh in the r_2-variable, we can adjust to it efficiently. However, should this feature run along a diagonal line, then, in order to approximate it well, we must have a fine mesh everywhere in r_1 and r_2. This means that we end up having a fine grid even in regions where the function to be approximated is quite smooth. For each function to be determined we at first carried out $n_{O_1O_2}$ one-dimensional spline fittings to have a regular mesh also in the symmetrized coordinate of the transfering proton. Then, the data on this regular mesh were fitted by tensor product bicubic splines.

As far as the evaluation of the restricted Hessian, twelve matrices of second derivatives of energy were computed at selected values of the reaction surface coordinates, and we obtained a global expression for such quantity through a bivariate four-point interpolation (see eq 3.1). The range for the interoxygen distance and the asymmetric stretching of the excess proton is 2.3−2.8 Å and −1.2−0.0 Å, respectively. Finally, the reaction surface parameters for the full process (i.e., for $-1.2 \le r_1 \le 1.2$) can be obtained by enforcing the identical atom symmetry.[15]

In Figure 3 we show the minimum energy surface. At the absolute minimum (C_2 point group) the proton is midway between the two oxygen atoms which are 2.378 Å apart. The potential acquires double-well characters only for O_1O_2 around 2.5 Å. The parametric dependence of Mulliken atomic net charges (obtained by using the MP2 density matrix) vs **r** is also reported (Figure 4). These quantities can be used in the evaluation of the solvent−complex V_{SC} potential. In fact, following Lobaugh and Voth,[31] such a potential can be expressed in terms of pairwise Lennard−Jones (LJ) and Coulomb interactions between various ionic sites. These interactions may be written as

$$V_{\text{pair}} = 4\epsilon\left[\left(\frac{\sigma}{R_{OO}}\right)^{12} - \left(\frac{\sigma}{R_{OO}}\right)^{6}\right] + \sum_m \sum_n \frac{Q_m Q_n}{R_{mn}} \quad (4.2)$$

where ϵ and σ are the usual Lennard−Jones parameters, and

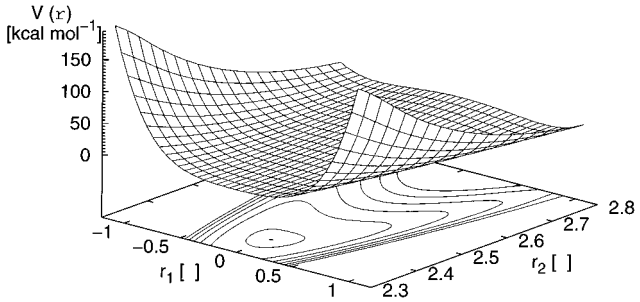

Figure 3. MP2/6-311G** minimum energy surface ($\bar{V}(\mathbf{r})$) for $H_5O_2^+$ dimer. The r_1 coordinate is the difference between the H_7O_1 and H_7O_2 lengths, while r_2 corresponds to O_1O_2 distance. The dot on the contour map identifies the minimum position; the level curves start from 0.3 kcal mol^{-1} and have 2 kcal mol^{-1} increments. The lengths are in angstroms.

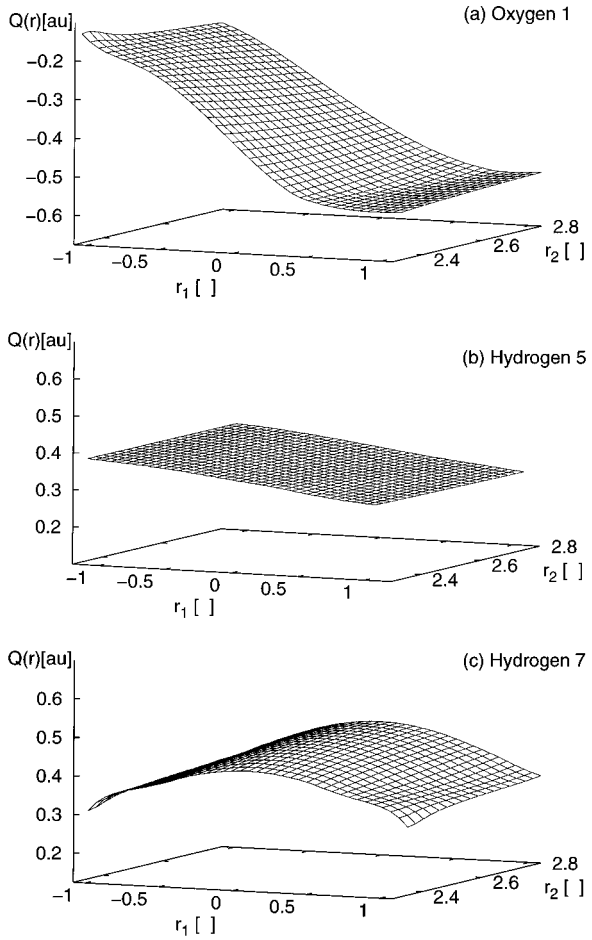

Figure 4. MP2/6-311G** Mulliken charges (Q) as a function of the proton transfer coordinate (r_1) and interoxygen distance (r_2) on (a) O_1, (b) H_5, and (c) H_7. Due to the nonlinearity of the hydrogen bond, the charge on H_6 is not equal to that on H_5. However the difference is too small to be appreciated on the plot scale. Charges on O_2, H_3, and H_4 are the mirror image of O_1, H_5, and H_6, respectively, about $r_1 = 0$. The lengths are in angstroms.

Q_m (Q_n) is the partial charge on the mth (nth) atom of the hydronium (water) located at a R_{mn} distance. The LJ interactions are only between oxygen atoms. The transfer of the proton between two molecular water hosts is accompanied by a considerable redistribution of charge, and one can mimic such an effect by considering the Q_m charges as functions only of the coordinates which are most effective during the proton transfer process, that is, the reaction surface variables **r**.

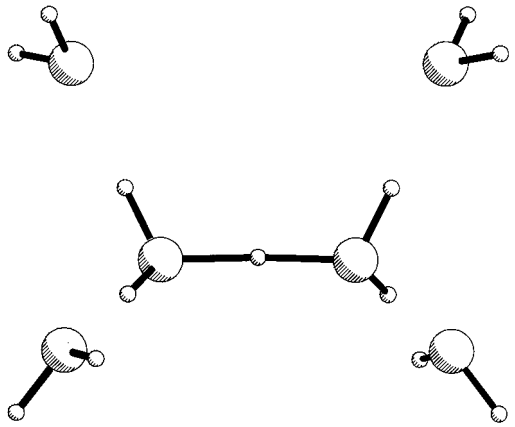

Figure 5. $H_5O_2^+$ complex solvated by four water molecules. The geometrical configuration shown corresponds to the MP2/6-311G** minimum.

To summarize, the knowledge of the functional form of the adiabatic reaction surface $\bar{V}$, quasi-equilibrium off-surface coordinates $\bar{\mathbf{u}}$, and restricted Hessian $\mathbf{V}^{(2)}_{\mathbf{uu}}$ allows the potential V_C in eq 4.1 to be specified. The solvent−complex V_{SC} potential can be determined once it is known how the atomic populations vary in the course of the reactive process, i.e., once the $\mathbf{Q}(\mathbf{r})$ are known. For the solvent−solvent potential V_{SS}, one could use, for example, the SPC water model[39] or more accurate models as they become available. Therefore the potential in eq 4.1 could be used for molecular dynamics simulation of the proton transfer process of the $H_5O_2^+$ dimer in the gas phase and in water and compared with experiment. These simulations will be carried out in the future to also help determine the global accuracy of the potential energy surface.

One comment is in order, however. Previous studies[40,41] on hydrated proton clusters have shown the importance of the nonclassical charge transfer effects in determining their stability. In the framework of the model, eq 4.1, used to mimic the total potential for the solvated $H_5O_2^+$ complex, one can take into account the charge transfer phenomenon by a well-tailored modification of the complex and complex−solvent water potentials. A way to do it is to use a "dressed" $H_5O_2^+$ complex, that is a dimer which is somehow prepared to interact with the solvent water. The practical procedure to follow has two steps: *i* and *j*. In the *i*-th step, one considers a discrete solvation model for the dimer where two equivalent water molecules are added, bonded by hydrogen bonds, to each of the two water molecules involved in the proton transfer (Figure 5). By carrying out *n* constrained optimizations on the solvated dimer, a set of quasi-equilibrium off-surface coordinates and atomic charges are obtained. In the *j*-th step one deals with the unsolvated dimer and computes energy, gradient, and Hessian at the geometrical configurations determined in the previous step which included additional water. The atomic charges from the *i*-th step can then be used in setting the V_{SC} potential. The complex potential V_C is, instead, obtained by taking the energy, gradient, and Hessian from the *j*-th step and quasi equilibrium coordinates from the *i*-th step. Furthermore, it should be pointed out that inclusion of quantum chemical reaction field models (see, e.g., refs 42−46) in the *i*-th step can lead to an improved description of electrostatic effects of the environment on the $H_5O_2^+$ complex. In such a way the bare dimer experiences not only a discrete but also a continuum-like interaction with the solvent waters.

The development of the dressed dimer potential will be subject of future work. Presently we have only performed preliminary calculations to ascertain that for the discrete solvated dimer, at the MP2/6-311G** level, the minimum configuration (obtained by optimizing all the degrees of freedom) still corresponds to an excess proton halfway between the O_1O_2 oxygens. In Table 1 we compare the values of the geometrical parameters at the minimum configuration for the isolated and partially solvated $H_5O_2^+$ complex. While the values of **r** coordinates are almost unaffected by the discrete solvation, sensible variations occur for those of the spectator coordinates. The invariance of the C_2 minimum configuration in the case of the solvated dimer can be ascribed to the balance between a charge stabilization and a charge transfer. In particular, the two waters interacting with the hydronium stabilize its excess charge so that its interaction with "$H_5O_2^+$ water" diminishes. Such an effect should lead to the shifting of the absolute minimum from a C_2 to a C_s configuration. However the other two waters transfer charges to the "$H_5O_2^+$ water", thus increasing its accepting capability.

5. Concluding Remarks

In the study of proton transfer reactions a feasible way to sample the configuration space within an *ab initio* framework is to determine the potential energy on a reaction surface where most of the reactive process takes place. Since such a surface is expected to play a dominant role in the dynamics, a global potential surface can be formulated in terms of harmonic deviations away from it. The applicability of such model rests on the development of an effective way to handle a large amount of data and to represent it in a flexible functional form. We therefore implemented a computational method based on spline fitting and bivariate interpolation and applied it to determine the global PES governing the proton transfer in the $H_5O_2^+$ dimer. This gas phase potential can be used as a core for determining the potential felt by the dimer when embedded in water. The missing information in such a case is the potential for dimer−solvent interactions. Since this quantity depends, among other things, on the charge distributions on the atoms involved in the proton transfer process, their pattern has been obtained in terms of bivariate functions of the interoxygen distance and of the asymmetric stretching for the excess proton.

The extension of the reaction surface model to large systems is limited by the difficulties in carrying out the necessary *ab initio* calculations of Hessian matrices at many points on the reaction surface. A good approximation of the force field away from the reaction surface can be obtained through the proper use of a method which yields a global potential by mixing local potentials in accordance to a minimum coupling principle. Therefore, a combined use of the reaction surface and minimum coupling method should offer a powerful tool to take explicitly into account the role of nonhydrogenic motions on the part of the configuration space which is spanned by a large polyatomic system during a proton transfer process. Furthermore, a global PES expressed in terms of the reaction surface approach for different reactive channels of a given system can be matched by a blending procedure. This also makes it possible to determine the PES governing proton hoppings along several donor/acceptor sites (i.e., a proton wire). Work is in progress on this topic.

Acknowledgment. This research was supported by a grant to G.A.V. from the National Institutes of Health (1R01-GM-53148). C.M. also acknowledges receipt of financial support from the NATO-CNR advanced fellowship program and the warm hospitality extended to her by G.A.V. and his group. We thank Marc Pavese, Amir Karger, and Giovanni Villani for their helpful comments on the manuscript.

Appendix A

Let us approximate the k-th diabatic potential by a second-order Taylor expansion about a minimum-like point $\mathbf{q}_k$. In order to simplify the following algebra we also expand it about the point $\mathbf{q}_{kl}$ to be used for determining the coupling term. Therefore one has

$$T_k(\mathbf{q}) = T_k(\mathbf{q}_{kl}) + \delta\mathbf{q}_{kl}^t\cdot\mathbf{T}_k^{(1)}(\mathbf{q}_{kl}) + {}^1/_2\delta\mathbf{q}_{kl}^t\cdot\mathbf{T}_k^{(2)}(\mathbf{q}_{kl})\cdot\delta\mathbf{q}_{kl} \quad \text{(A1)}$$

The $\mathbf{T}_k^{(n)}$ coefficients are easily derived from the ones of the Taylor expansion about $\mathbf{q}_k$; namely, they are:

$$T_k(\mathbf{q}_{kl}) = V_k(\mathbf{q}_k) + (\mathbf{q}_{kl} - \mathbf{q}_k)^t\cdot\mathbf{V}_k^{(1)}(\mathbf{q}_k) + {}^1/_2(\mathbf{q}_{kl} - \mathbf{q}_k)^t\cdot\mathbf{V}_k^{(2)}(\mathbf{q}_k)\cdot(\mathbf{q}_{kl} - \mathbf{q}_k)$$

$$\mathbf{T}_k^{(1)}(\mathbf{q}_{kl}) = \mathbf{V}_k^{(1)}(\mathbf{q}_k) + (\mathbf{q}_{kl} - \mathbf{q}_k)^t\cdot\mathbf{V}_k^{(2)}(\mathbf{q}_k)$$

$$\mathbf{T}_k^{(2)}(\mathbf{q}_{kl}) = \mathbf{V}_k^{(2)}(\mathbf{q}_k)$$

Then, substituting eq A1 and the analogous one for the l-th cell potential in eq 3.8, one obtains the square of the coupling function

$$\begin{aligned} B_{kl} = {} & [T_k(\mathbf{q}_{kl}) - V(\mathbf{q}_{kl})][T_l(\mathbf{q}_{kl}) - V(\mathbf{q}_{kl})] + \\ & [T_k(\mathbf{q}_{kl}) - V(\mathbf{q}_{kl})]\delta\mathbf{q}_{kl}^t\cdot[\mathbf{T}_l^{(1)}(\mathbf{q}_{kl}) - \mathbf{V}^{(1)}(\mathbf{q}_{kl})] + \\ & [T_l(\mathbf{q}_{kl}) - V(\mathbf{q}_{kl})]\delta\mathbf{q}_{kl}^t\cdot[\mathbf{T}_k^{(1)}(\mathbf{q}_{kl}) - \mathbf{V}^{(1)}(\mathbf{q}_{kl})] + \\ & {}^1/_2[T_k(\mathbf{q}_{kl}) - V(\mathbf{q}_{kl})]\delta\mathbf{q}_{kl}^t\cdot[\mathbf{T}_l^{(2)}(\mathbf{q}_{kl}) - \mathbf{V}^{(2)}(\mathbf{q}_{kl})]\cdot\delta\mathbf{q}_{kl} + \\ & {}^1/_2[T_l(\mathbf{q}_{kl}) - V(\mathbf{q}_{kl})]\delta\mathbf{q}_{kl}^t\cdot[\mathbf{T}_k^{(2)}(\mathbf{q}_{kl}) - \mathbf{V}^{(2)}(\mathbf{q}_{kl})]\cdot\delta\mathbf{q}_{kl} + \\ & \{[\mathbf{T}_l^{(1)}(\mathbf{q}_{kl}) - \mathbf{V}^{(1)}(\mathbf{q}_{kl})]\cdot\delta\mathbf{q}_{kl}^t\}\{[\mathbf{T}_k^{(1)}(\mathbf{q}_{kl}) - \mathbf{V}^{(1)}(\mathbf{q}_{kl})]\cdot\delta\mathbf{q}_{kl}^t\} \end{aligned} \quad \text{(A2)}$$

This result has been derived by Chang and Miller[11] for a two-state problem, however it should be emphasized that it holds for any number of states, due to the general validity of eq 3.8 in the limit of pairwise couplings for diabatic potentials.

At this point one would like this function to have a better asymptotic behavior, i.e., to go smoothly to zero as it approaches the extrema of the interval in which is defined. This can be accomplished if B_{kl} has the shape of a polydimensional Gaussian function. One therefore must transform eq A2 from a polynomial into a Gaussian in the $\delta\mathbf{q}_{kl}$ variable

$$B_{kl} = A_{0_{kl}}\exp[\delta\mathbf{q}_{kl}^t\cdot\mathbf{A}_{1_{kl}} - \delta\mathbf{q}_{kl}^t\cdot\mathbf{A}_{2_{kl}}\cdot\delta\mathbf{q}_{kl}] \quad \text{(A3)}$$

The coefficients of this Gaussian can be obtained by performing a cumulant resummation.

Let us for simplicity consider a generic second-degree polynomial in x

$$F(x) = a_0 + b_1x + b_2x^2 \quad \text{(A4)}$$

which one would express as

$$G(x) = a_0\exp(a_1x + a_2x^2) \quad \text{(A5)}$$

One can get the desidered coefficients a_i by expanding the exponential function in a power series

$$G(x) \approx a_0(1 + a_1x + {}^1/_2a_1^2x^2 + ... + a_2x^2 + ...) \quad \text{(A6)}$$

and equating the coefficients of eq A4 and eq A6 corresponding to the same powers of x. The yields the following expression for the a_i terms

$$a_1 = \frac{b_1}{a_0} \qquad a_2 = \frac{b_2}{a_0} - {}^1/_2\left(\frac{b_1}{a_0}\right)^2 \quad \text{(A7)}$$

This procedure applied to eq A2 and eq A3 gives:

$$A_{0_{kl}} = [T_k(\mathbf{q}_{kl}) - V_{kl}(\mathbf{q}_{kl})][T_l(\mathbf{q}_{kl}) - V_{kl}(\mathbf{q}_{kl})] \quad \text{(A8a)}$$

$$\mathbf{A}_{1_{kl}} = \frac{\mathbf{T}_k^{(1)}(\mathbf{q}_{kl}) - \mathbf{V}_{kl}^{(1)}(\mathbf{q}_{kl})}{T_k(\mathbf{q}_{kl}) - V_{kl}(\mathbf{q}_{kl})} + \frac{\mathbf{T}_l^{(1)}(\mathbf{q}_{kl}) - \mathbf{V}_{kl}^{(1)}(\mathbf{q}_{kl})}{T_l(\mathbf{q}_{kl}) - V_{kl}(\mathbf{q}_{kl})} \quad \text{(A8b)}$$

$$\begin{aligned} \mathbf{A}_{2_{kl}} = {} & \frac{[\mathbf{T}_k^{(1)}(\mathbf{q}_{kl}) - \mathbf{V}_{kl}^{(1)}(\mathbf{q}_{kl})]\cdot[\mathbf{T}_k^{(1)}(\mathbf{q}_{kl}) - \mathbf{V}_{kl}^{(1)}(\mathbf{q}_{kl})]^t}{[T_k(\mathbf{q}_{kl}) - V_{kl}(\mathbf{q}_{kl})]^2} + \\ & \frac{\mathbf{V}_{kl}^{(2)}(\mathbf{q}_{kl}) - \mathbf{T}_k^{(2)}(\mathbf{q}_{kl})}{T_k(\mathbf{q}_{kl}) - V_{kl}(\mathbf{q}_{kl})} + \\ & \frac{[\mathbf{T}_l^{(1)}(\mathbf{q}_{kl}) - \mathbf{V}_{kl}^{(1)}(\mathbf{q}_{kl})]\cdot[\mathbf{T}_l^{(1)}(\mathbf{q}_{kl}) - \mathbf{V}_{kl}^{(1)}(\mathbf{q}_{kl})]^t}{[T_l(\mathbf{q}_{kl}) - V_{kl}(\mathbf{q}_{kl})]^2} + \\ & \frac{\mathbf{V}_{kl}^{(2)}(\mathbf{q}_{kl}) - \mathbf{T}_l^{(2)}(\mathbf{q}_{kl})}{T_l(\mathbf{q}_{kl}) - V_{kl}(\mathbf{q}_{kl})} \end{aligned} \quad \text{(A8c)}$$

Appendix B

If the matrix representation of $\hat{v}$ is

$$\begin{bmatrix} T_k & C_{kl} \\ C_{kl} & T_l \end{bmatrix} \quad \text{(B1)}$$

then the minimum coupling potential V_{MC} is

$$V_{\mathrm{MC}} = S_{kl} - [D_{kl}D_{kl} + B_{kl}]^{1/2} \quad \text{(B2)}$$

with B_{kl} given by eq A3. The $\mathbf{S}_{kl}^{(n)}$ and $\mathbf{D}_{kl}^{(n)}$ terms (with $n = 0$, 1, 2) are defined as

$$\mathbf{S}_{kl}^{(n)} = \frac{\mathbf{T}_k^{(n)} + \mathbf{T}_l^{(n)}}{2} \qquad \mathbf{D}_{kl}^{(n)} = \frac{\mathbf{T}_k^{(n)} - \mathbf{T}_l^{(n)}}{2} \quad \text{(B3)}$$

where $\mathbf{T}_k^{(n)}$ and $\mathbf{T}_l^{(n)}$ are the n-th derivatives of the k-th and l-th cell potentials, respectively, and they are tensors of rank n. Note that the scalars S_{kl} and D_{kl} are given by $\mathbf{S}_{kl}^{(0)}$ and $\mathbf{D}_{kl}^{(0)}$, respectively.

The functional expression for the minimum coupling energy gradient $V^{(1)}{}_{\mathrm{MC}}$ and Hessian $V^{(2)}{}_{\mathrm{MC}}$ can be obtained by taking the first and second derivatives of eq B2 vs $\mathbf{q}$. They are given by

$$\mathbf{V}^{(1)}{}_{\mathrm{MC}} = \mathbf{S}_{kl}^{(1)} - [D_{kl}D_{kl} + B_{kl}]^{-1/2}[D_{kl}\mathbf{D}_{kl}^{(1)} + {}^1/_2\mathbf{B}_{kl}^{(1)}] \quad \text{(B4)}$$

and

$$\begin{aligned} \mathbf{V}^{(2)}{}_{\mathrm{MC}} = {} & \mathbf{S}_{kl}^{(2)} + [D_{kl}D_{kl} + B_{kl}]^{-3/2}[D_{kl}\mathbf{D}_{kl}^{(1)} + {}^1/_2\mathbf{B}_{kl}^{(1)}]\cdot \\ & [D_{kl}\mathbf{D}_{kl}^{(1)} + {}^1/_2\mathbf{B}_{kl}^{(1)}]^t - [D_{kl}D_{kl} + B_{kl}]^{-1/2}[D_{kl}\mathbf{D}_{kl}^{(2)} + \\ & \mathbf{D}_{kl}^{(1)}\cdot\mathbf{D}_{kl}^{(1)^t} + {}^1/_2\mathbf{B}_{kl}^{(2)}] \end{aligned} \quad \text{(B5)}$$

respectively. The $\mathbf{B}_{kl}^{(1)}$ and $\mathbf{B}_{kl}^{(2)}$ quantities entering in the above equations are defined as

$$\mathbf{B}_{kl}^{(1)} = B_{kl}[\mathbf{A}_{1_{kl}} - \mathbf{A}_{2_{kl}} \cdot \delta\mathbf{q}_{kl}] \tag{B6}$$

and

$$\mathbf{B}_{kl}^{(2)} = \mathbf{B}_{kl}^{(1)} \cdot [\mathbf{A}_{1_{kl}} - \mathbf{A}_{2_{kl}} \cdot \delta\mathbf{q}_{kl}]^t - B_{kl}\mathbf{A}_{2_{kl}} \tag{B7}$$

respectively, with $\mathbf{A}_{m_{kl}}$ coefficients from eqs A8.

References and Notes

(1) *Potential Energy Surfaces and Dynamics Calculations*; Truhlar, D. G., Ed.; Plenum: New York, 1981.
(2) Murrell, J. N.; Carter, S.; Farantos, S. C.; Huxley, P.; Varandas, A. J. C. *Molecular Potential Energy Functions*; Wiley: New York, 1984.
(3) Hirst, D. M. *Potential Energy Surfaces*; Taylor and Francis: London, 1985.
(4) Truhlar, D. G.; Steckler, R.; Gordon, M. S. *Chem. Rev.* **1987**, *87*, 217.
(5) Schatz, G. C. *Rev. Mod. Phys.* **1989**, *61*, 669.
(6) Primas, H. *Chemistry, Quantum Mechanics and Reductionism: Perspectives in Theoretical Chemistry*, 2nd ed.; Springer-Verlag: Berlin, 1983.
(7) Heidrich, D. *The Reaction Path in Chemistry*; Vol. 16 of Understanding Chemical Reactivity, Vol. 16; Kluwer: Dordrecht, The Netherlands, 1995.
(8) Marcus, R. A. *J. Chem. Phys.* **1966**, *45*, 4493.
(9) Fukui, K. *J. Phys. Chem.* **1970**, *74*, 4161.
(10) Miller, W. H.; Handy, N. C.; Adams, J. E. *J. Chem. Phys.* **1980**, *72*, 99.
(11) Chang, Y. T.; Miller, W. H. *J. Phys. Chem.* **1990**, *94*, 5884.
(12) Chang, Y. T.; Minichino, C.; Miller, W. H. *J. Chem. Phys.* **1992**, *96*, 4341.
(13) Ischtwan, J.; Collins, M. J. *J. Chem. Phys.* **1994**, *100*, 8080.
(14) Nguyen, K. A.; Rossi, I.; Truhlar, D. G. *J. Chem. Phys.* **1995**, *103*, 5522.
(15) Jordan, M. J. T.; Thompson, K. C.; Collins, M. J. *J. Chem. Phys.* **1995**, *102*, 5647.
(16) Carrington, T.; Jr.; Miller, W. H. *J. Chem. Phys.* **1986**, *84*, 4364.
(17) Hoffman, D. K.; Nord, R. S.; Ruedenberg, K. *Theor. Chim. Acta* **1986**, *69*, 265.
(18) Quapp, W. *Theor. Chim. Acta* **1989**, *75*, 447.
(19) Basilevski, M. V. *Chem. Phys.* **1982**, *67*, 337.
(20) Wilson, E. B., Jr.; Decius, J. C.; Cross, P. C. *Molecular Vibrations*; McGraw-Hill: New York, 1955.
(21) Califano, S. *Vibrational States*; Wiley: New York, 1976.
(22) Shida, N.; Barbara, P. F.; Almlöf, J. *J. Chem. Phys.* **1991**, *94*, 3633.
(23) de Boor, C. *A Practical Guide to Splines*; Springer-Verlag: New York, 1978.
(24) Dierckx, P. *Curve and Surface Fitting with Splines*; Oxford University Press: New York, 1993.
(25) Abramowitz, M.; Stegun, I. A. *Handbook of Mathematical Functions*; Dover: New York, 1964; p 882.
(26) Warshel, A.; Weiss, R. M. *J. Am. Chem. Soc.* **1980**, *102*, 6218.
(27) Fukui, K. In *The World of Quantum Chemistry*; Daudel, R., Pullman, B., Eds.; Reidel, Dordrecht, The Netherlands, 1974; p 113.
(28) Fukui, K. *Acc. Chem. Res.* **1981**, *14*, 368.
(29) Frisch, M. J.; Trucks, G. W.; Schlegel, H. B.; Gill, P. M. W.; Johnson, B. G.; Robb, M. A.; Cheeseman, J. R.; Keith, T.; Petersson, G. A.; Montgomery, J. A.; Raghavachari, K.; Al-Laham, M. A.; Zakrzewski, V. G.; Ortiz, J. V.; Foresman, J. B.; Cioslowski, J.; Stefanov, B. B.; Nanayakkara, A.; Challacombe, M.; Peng, C. Y.; Ayala, P. Y.; Chen, W..; Wong, M. W.; Andres, J. L.; Replogle, E. S.; Gomperts, R.; Martin, R. L.; Fox, D. J.; Binkley, J. S.; Defrees, D. J.; Baker, J.; Stewart, J. P.; Head-Gordon, M.; Gonzalez, C.; Pople, J. A. *Gaussian 94*; Gaussian Inc.: Pittsburgh, PA, 1994.
(30) Zundel, G. In *The Hydrogen Bond: Recent Developments in Theory and Experiment*; Schuster, G. Z. P., Sandorfy, C., Eds.; North Holland: Amsterdam, 1976; Vol. 2.
(31) Lobaugh, J.; Voth, G. A. *J. Chem. Phys.* **1996**, *104*, 2056.
(32) Newton, M. D.; Ehrenson, S. *J. Am. Chem. Soc.* **1971**, *93*, 4971.
(33) Scheiner, S. *J. Am. Chem. Soc.* **1981**, *103*, 315.
(34) Scuseria, G. E. *J. Chem. Phys.* **1991**, *94*, 442.
(35) Xie, Y.; Remington, B.; Schaefer, H. F., III *J. Chem. Phys.* **1994**, *101*, 4878.
(36) Latajka, Z.; Scheiner, S. *J. Mol. Struct. (THEOCHEM)* **1991**, *234*, 4391.
(37) Krishan, R.; Binkley, J. S.; Seeger, R.; Pople, J. A. *J. Chem. Phys.* **1980**, *72*, 650.
(38) Del Bene, J. E. *J. Comput. Chem.* **1987**, *8*, 810.
(39) Berendson, H. J. C.; Postma, J. P. M.; van Gusteren, W. F.; Hermans, J. J. In *Intermolecular Forces*; Pullman, B., Ed.; Reidel: Dordrecht, The Netherlands, 1981.
(40) Komatsuzaki, T.; Ohmine, I. *Chem. Phys.* **1994**, *180*, 239.
(41) Tortonda, F. R.; Pascual-Ahuir, J. L.; Silla, E.; Tuñón, I. *J. Phys. Chem.* **1993**, *97*, 11087.
(42) Rivail, J. L.; Rinaldi, D. *Chem. Phys.* **1976**, *18*, 2333.
(43) Miertus, S.; Scrocco, E.; Tomasi, J. *Chem. Phys.* **1981**, *55*, 117.
(44) Tapia, O.; Goscinski, O. *Mol. Phys.* **1975**, *29*, 1653.
(45) Tapia, O. *Theor. Chim. Acta* **1978**, *47*, 157.
(46) Wong, M. W.; Wiberg, K. B.; Frisch, M. *J. Chem. Phys.* **1991**, *95*, 8991.